

1 **Title: An Automated Classification Method for Single Sweep Local Field Potentials**
2 **Recorded from Rat Barrel Cortex under Mechanical Whisker Stimulation**

3
4 Author list: Mufti Mahmud^{1,4}, Davide Travalin², Alessandra Bertoldo³, Stefano Girardi¹, Marta
5 Maschietto¹, Stefano Vassanelli^{1,*}

6
7 Affiliation of authors:

8 ¹NeuroChip Laboratory, Dept. of Human Anatomy & Physiology, University of Padova, 35131
9 Padova, Italy

10 ²During the work author was with: Dept. of Information Engineering, University of Padova,
11 35131 Padova, Italy. Now: Clinical Department, St. Jude Medical Italia S.p.A, 20864 Agrate
12 Brianza, Italy

13 ³Dept. of Information Engineering, University of Padova, 35131 Padova, Italy

14 ⁴Institute of Information Technology, Jahangirnagar University, Savar, 1342 Dhaka, Bangladesh

15

16

17 Running title: **Automated Classification of Single Sweep Local Field Potentials**

18

19 *Corresponding author: Stefano Vassanelli

20 Tel: +39 049 8275337

21 Fax: +39 049 8275301

22 E-mail: stefano.vassanelli@unipd.it

23

24 **ABSTRACT**

25 Understanding brain signals as an outcome of brain's information processing is a
26 challenge for the neuroscience and neuroengineering community. Rodents sense and explore the
27 environment through whisking. The local field potentials (LFPs) recorded from the barrel
28 columns of the rat somatosensory cortex (S1) during whisking provide information about the
29 tactile information processing pathway. Particularly when using large-scale high-resolution
30 neuronal probes, during each experiment many single LFPs are recorded as an outcome of
31 underlying neuronal network activation and averaged to extract information. However, single
32 LFP signals are frequently very different from each other and extracting information provided by
33 their shape is a useful way to better decode information transmitted by the network. In this work,
34 we propose an automated method capable of classifying these signals based on their shapes. We
35 used template matching approach to recognize single LFPs and extracted the contour information
36 from the recognized signal to generate a feature matrix, which is then classified using the
37 intelligent K-means clustering. As an application example, shape specific information (e.g.,
38 latency, and amplitude) of LFPs evoked in the rat somatosensory barrel cortex and used in
39 decoding the rat whiskers information processing pathway is provided by the method.

40

41

42

43 Keywords: Local field potentials, Barrel cortex, Whisker stimulation, LFP classification,
44 Neuronal signal analysis

45

46 **1. Introduction**

47 During the last decade many researchers took their interest in deciphering brain activity
48 as an outcome of the activation of underlying neuronal networks. To do so, they have developed
49 high resolution neuronal probes capable of providing unprecedented information about neuronal
50 circuits [1]. These recording tools deliver huge amount of recordings containing spiking activity
51 as well as field potentials generated in the brain area under investigation. To understand the
52 signal propagation among different cortical layers and the information processing pathways,
53 scientists have relied on the local field potentials (LFPs). Due to the fact that the scientists use
54 stimulus–locked field potentials to assess and understand the effect of stimuli on a brain area(s),
55 the LFPs provide a ‘fingerprint’ of the stimuli’s effect on activity propagation in neuronal
56 networks of the brain region under study [2]. The conventional way of analyzing these LFPs is to
57 record for a period of time and then obtain a stimulus–locked average. However, experimental
58 studies have shown that the individual information provided by a single sweep may disappear if
59 one considers an average over several runs under the same stimulus conditions [3]. Furthermore,
60 to understand certain issues of the brain (for example, signal processing pathway and cortical
61 layer activation order [8]) and for certain operations (for example, current source density analysis)
62 signal shape plays an important role [4]. It is thus implied that different shapes in the single
63 sweep signals denote different neuronal network activity. Therefore, a shape based classification
64 method is required to extract different LFP shapes present in a pool of single LFPs to decipher
65 the neuronal network activity from the LFPs. A wide range of research has been conducted in
66 detection and sorting of neuronal spikes [5], but till date there is no method capable of
67 performing similar sorting for the single LFPs.

68 In this work, we present a method for single LFPs classification based on the shape of the
69 signals. This method exploits information about the signal contour to perform the classification.
70 The terms classification, signal sorting and clustering will be used synonymously throughout the
71 text.

72 As the method uses the shape information of the LFPs for the classification, it is worth
73 taking a look to the contour characteristics of the signals. The LFPs recorded from a barrel
74 column of the rat S1 cortex by stimulating the corresponding whisker can be differentiated by
75 their specific characteristics based on the depth or layer they are recorded from, thanks to the
76 existing research on the rat barrel cortex. Figure 1 shows a depth profile during one of our
77 experiments. The signals were recorded equidistantly at 90 μm pitch from the cortical surface to
78 deep cortical layer, but only representative signals from each layer are shown.

79 As illustrated by Ahrens and Kleinfeld [6] and Kublik [7], the cortical LFPs can be
80 characterized by four consecutive events. Event 1 (E1): a small positive / negative peak; event 2
81 (E2): a dominant negative peak; event 3 (E3): a slow positive peak; and event 4 (E4): a slow
82 negative peak. Usually in upper cortical layers (I, II) the signals are expected to have positive E1
83 followed by the E2, E3 and E4. In the signals recorded from the middle layers (III, IV, and V)
84 the E1 is absent and they are expected to have the E2, followed by the E3 and E4. In deeper brain
85 cortex (layer VI), the E2 becomes smaller and usually gets divided into two smaller negative
86 peaks (negative E1, and E2), followed by E3 and E4 [8]. These characteristics of the signals and
87 with the a priori information about the recording position are used in generation of the template.

88 The single signal sorting is done in four steps: (1) smoothing of single LFPs within
89 individual recording sweeps; (2) template generation; (3) single LFP recognition through

90 template matching and (4) clustering of recognized single signals. The smoothing is performed
91 using nonlinear least square estimation to remove the spatial oscillations and noise in the single
92 LFPs. Once the signals are estimated, for each signal the starting and end of the response is
93 determined as the stimulus–onset and end of signal, respectively. An average of the response part
94 is considered as a template to be used for signal recognition. This method matches the contour of
95 the template for recognition of the single signals which is compared to each of the single LFP's
96 contour with a predefined boundary condition. If the single LFP falls within the boundary
97 condition, the single signal is considered to be recognized. Once the single LFP recognition is
98 over, intelligent K–means clustering is applied on the recognized LFPs to classify them
99 according to their shapes. The classified or clustered single LFPs are then locally averaged. In
100 agreement with previously reported results [9] averaged local LFPs show different shape and
101 amplitude characterizing those signals. These parameters provide insights about underlying
102 neuronal network activity and on the whiskers signal processing pathways. However, clustered
103 averages of the single LFPs revealed differences in event latencies and amplitudes, thus
104 demonstrating differentiated network activity within the same cortical area at different times but
105 after the same stimulus.

106 **2. Materials and Methods**

107 **I. Clustering Method**

108 *A. Template Generation*

109 The first step of the template generation is smoothing. As the single LFPs contain
110 spontaneous neural oscillations and noise, it is often difficult to have precise information about
111 the individual signal events. Thus, removal of oscillations and noise is required. In case of spike

112 signals detection it would be possible to use a high pass filter to get rid of slow oscillations, but
 113 as our signals contain mainly LFPs (in the range of 1 to 100 Hz) using a simple filter will distort
 114 the response. Therefore, we removed oscillations and noise through smoothing / estimation using
 115 the Gauss–Newton based nonlinear least square method.

116 To estimate the single sweep signals we considered a generalized measurement error
 117 based model (eq. 1).

$$\begin{aligned}
 118 \quad x_k &= y_k + v_k \\
 119 \quad \Rightarrow x_k &= g(t_k, \mathbf{x}^*) + v_k \qquad (1)
 \end{aligned}$$

120 where the model parameter, $\mathbf{x}^* = [x^*_1, x^*_2, \dots, x^*_M]^T$ is a vector and t is the time, with $k=1, \dots, N$
 121 and N being the total data points present in a single sweep signal. As per this model, the recorded
 122 signal at time t_k is an integrated sum of the model's response (y_k) and the measurement error (v_k),
 123 under the assumption that the measurement error is additive, zero mean and Gaussian in
 124 distribution. It is further assumed that time is the only independent variable and the
 125 measurements are done precisely at known times, t_k .

126 The estimation parameter vector is calculated based on the minimization of the prediction
 127 error, $e(\mathbf{x}^*)$. When the true value of \mathbf{x}^* is unknown, a generic value of \mathbf{x}^* is used that minimizes
 128 the difference between the data vector and the model prediction for that particular value of \mathbf{x}^* ,
 129 i.e., $e(\mathbf{x}^*) = \mathbf{x} - g(t, \mathbf{x}^*)$. The optimal \mathbf{x}^* value is chosen iteratively based on the smallest
 130 possible value of $e(\mathbf{x}^*)$. The goodness of the chosen \mathbf{x}^* value is thus given by the Euclidean
 131 norm of a generic vector $R = [r_1, \dots, r_N]^T$ and is given by:

132
$$\|R\|^2 = \mathbf{r}^T \mathbf{r} = \sum_{i=1}^N r_i^2$$

133 And the weighted Euclidean norm is given by:

134
$$\|R\|_{\Phi}^2 = \mathbf{r}^T \Phi \mathbf{r} = \sum_{i=1}^N \frac{r_i^2}{\Phi_i}$$

135 where Φ is defined as a positive square matrix of $N \times N$ dimension.

136 If the above formalism of parameter estimation fails to provide satisfactory smoothing, a
 137 non-linear least square method is used, which is more effective, but computationally expensive.
 138 This validation is done through detection of the prestimulus part of a signal and comparing the
 139 standard deviation before and after smoothing. It has been empirically found that if the
 140 difference of standard deviations between pre- and post-smoothing is more than half of the
 141 standard deviation of the original signal, a more sophisticated smoothing technique is required.

142 From the definition of least square [10], for a given vector function $f(x): \mathbb{R}^n \mapsto \mathbb{R}^m$ with
 143 $m \geq n$, we want to minimize the norm of the function $\|f(x)\|$ or equivalently find:

144
$$x^* = \operatorname{argmin}_x \{F(x)\} \tag{2}$$

145 Where x^* is a local minimizer for $F(x)$ meaning that for a set of arguments x^* , the $F(x)$ is kept
 146 minimal within a range δ , with δ being a small positive number.

147
$$F(x) = \frac{1}{2} \sum_{i=1}^m (f_i(x))^2 = \frac{1}{2} \|f(x)\|^2 = \frac{1}{2} f(x)^T f(x) \tag{3}$$

148 Now adding a weight function (the covariance matrix of the prediction error, Σ_v) to eq. 3
 149 and rewriting the model of eq. 1 to eq. 4 to calculate the prediction error, an analytical solution
 150 of the problem (in eq. 5) can be obtained.

$$151 \quad x = y(x^*) + v$$

$$152 \quad (4)$$

$$153 \quad x^* = (y^T \Sigma_v^{-1} y)^{-1} y^T \Sigma_v^{-1} x \quad (5)$$

154 where y is the model prediction with x^* set of parameters and x is the actual measured values.

155 To solve the nonlinearity, the initial value at $x_k^*, k = 0$ is assigned to the parameter vector.
 156 Then, the model is linearized around the initial value using the first order Taylor's expansion.
 157 Thus the problem can be represented by eq. 6.

$$158 \quad \Delta x = P \Delta x^* + v \quad (6)$$

159 where P is a partial derivative matrix of $N \times M$ size with predicted values using the initial
 160 condition ($x_k^*, k = 0$).

161 Now, the linear formula can be used to estimate the parameters as in eq. 7 and a new
 162 parameter vector is obtained by eq. 8. This iterative process is repeated until the cost function
 163 stabilizes or falls below a threshold.

$$164 \quad \Delta x^* = (P^T \Sigma_v^{-1} P)^{-1} P^T \Sigma_v^{-1} x \quad (7)$$

$$165 \quad x_{k+1}^* = x_k^* + \Delta x_k^* \quad (8)$$

166 The estimated signals are scanned for occurrence of the aforementioned events. In usual
 167 cases, the stimulus-onset defines the starting point and the end of response defines the end of the
 168 template. As all the signals don't have the same end of response, signals are zero-padded and
 169 averaged to obtain a template.

170 *B. Single Sweep Recognition*

171 Once the template is generated, the contour of the template is used to recognize the single
 172 signals. Boundary conditions (lower and upper bounds) are imposed to facilitate the recognition
 173 process and for calculating the boundary conditions.

$$174 \quad V_{tmp} = \frac{1}{N} \sum_{i=1}^N [Sw_i(k) - Temp(k)]^2 \quad (9)$$

175 where Sw is the zero-padded and truncated single LFPs and $Temp$ is the template.

176 The upper and lower bounds are calculated using eq. 10 and eq. 11.

$$177 \quad Up(k) = Temp(k) + (a * (V_{tmp}(k))^{1/2} + b) \quad (10)$$

$$178 \quad Low(k) = Temp(k) - (a * (V_{tmp}(k))^{1/2} + b) \quad (11)$$

179 where a , b are constant; the values of a , b ($a = STD(Temp)$, and $b = 3*STD(Temp)$) are
 180 determined empirically and STD standing for standard deviation.

181 A signal is considered as recognized (following the contour of the template), if and only
 182 if all of its data points lie within the range of the boundary conditions.

183 *C. Clustering the Recognized LFPs*

184 Once the single LFP signals are recognized, they are individually scanned for events (E1–
 185 E4) that characterize the LFPs. For this event detection purpose we used an *in-house* algorithm
 186 [8]. These shape characterizing events of the signal recorded from a particular cortical position
 187 are used to form the feature matrix to be clustered. For our clustering algorithm we used a feature
 188 matrix of size $200 \times N$, i.e., from each single sweep we extracted 200 points related to the events.
 189 However, as the shape information is important for the clustering, these 200 points were not
 190 selected as evenly distributed among the whole signal; rather more points were selected around
 191 the events to represent the signal shape characteristics at a higher resolution.

192 For our purpose of clustering we used the ‘intelligent K–means method’ of classifying
 193 the feature matrix generated from the recognized LFPs, which is an updated version of the
 194 classical K–means method [11–12].

195 The K–means method usually is applied to a dataset involving a set of N entities, I , a set
 196 of M features, V , and an entity–to–feature matrix $Y=(y_{iv})$, where y_{iv} is the value of feature $v \in V$ at
 197 entity $i \in I$. The method produces a partition $S=\{S_1, S_2, \dots, S_K\}$ of I in K non–overlapping classes
 198 S_k , referred to as clusters, each with a centroid $c_k=(c_{kv})$, an M –dimensional vector in the feature
 199 space ($k=1, 2, \dots, K$). Centroids form set $C=\{c_1, c_2, \dots, c_K\}$. The criterion, minimized by the method,
 200 is the within–cluster summary distance to centroids:

$$201 \quad W(S, C) = \sum_{k=1}^K \sum_{i \in S_k} d(i, c_k) \quad (12)$$

202 where d is the squared Euclidean distance.

203 Given K M –dimensional vectors c_k as cluster centroids, the algorithm updates clusters S_k
 204 according to the Minimum distance rule: for each entity i in the data table, its distances to all

205 centroids are calculated and the entity is assigned to its nearest centroid. Given the clusters S_k ,
206 centroids c_k are updated according to the distance d in eq. 12, $k=1, 2, \dots, K$. Specifically, c_k is
207 calculated as the vector of within-cluster averages as d in eq. 12 is the squared Euclidean
208 distance. This process is reiterated until clusters S_k stabilize.

209 However, this approach has as a severe drawback that the cluster number, K , is required
210 to be supplied before start of the classification. To overcome this, we adapted the intelligent K-
211 Means (*i*K-Means) clustering method as proposed in [13]. This *i*KMeans method uses an
212 anomalous pattern (AP) to find out the appropriate number of clusters.

213 The AP algorithm starts from an entity, which is the farthest from the origin, as the initial
214 centroid c . After that, a one-cluster version of the generic K-Means is used. The current AP
215 cluster S is defined as the set of all those entities that are closer to c than to the origin, and the
216 next centroid c is defined as the center of gravity of S . This process is iterated until convergence.

217 Finally, when the single LFPs are classified into their respective clusters, they are
218 cluster-wise averaged for further processing.

219 **II. Neurosurgery and Signal Acquisition**

220 *A. Animal Preparation*

221 All procedures followed Italian Ministry of Health Guidelines and were approved by the
222 Ethical Committee of the University of Padova, Italy. P30–P40 male rats were anesthetized with
223 an induction mixture of Tiletamine (2 mg/100 g weight) and Xylazine (1.4 g/100 g weight). The
224 anesthesia level was monitored throughout the experiment by testing eye and hind-limb reflexes,
225 respiration and checking the absence of whiskers' spontaneous movements. Whenever necessary,

226 additional doses of Tiletamine (0.5 mg/100 g weight) and Xylazine (0.5 g/100 g weight) were
227 provided.

228 During the surgery and the recording section, animals were kept on a common stereotaxic
229 apparatus under a stereomicroscope and fixed by teeth- and ear-bars. The body temperature was
230 constantly monitored with a rectal probe and maintained at about 37°C using a homeothermic
231 heating pad. Heart beat was assessed by standard ECG. To expose the cortical area of interest,
232 anterior-posterior opening in the skin was made along the medial line of the head, starting from
233 the imaginary eyeline and ending at the neck. While the skin was kept apart using halsted-
234 mosquito hemostats forceps, the connective tissue between skin and skull was gently removed by
235 means of a bone scraper. Thus, the skull over the right hemisphere was drilled to open a window
236 in correspondence of the S1 cortex (-1 ÷ -4 AP, +4 ÷ +8 ML) [14]. Meninges were then
237 carefully cut by means of forceps at coordinates -2.5 AP, +6 LM for the subsequent insertion of
238 the recording micropipette.

239 Throughout experiment, the brain was bathed by a standard Kreb's solution (in mM:
240 NaCl 120, KCl 1.99, NaHCO₃ 25.56, KH₂PO₄ 136.09, CaCl₂ 2, MgSO₄ 1.2, glucose 11),
241 constantly oxygenated and warmed at 37° C. At the end of the surgery, contralateral whiskers
242 were trimmed at about 10 mm from the mystacial pad.

243 *B. Whiskers Stimulation and Recording*

244 The recording of LFPs from S1 was performed by means of borosilicate micropipettes (1
245 MΩ resistance), filled with Kreb's solution. The pipette was fixed to a micromanipulator at 45°-
246 tilted respect to the vertical axis of the manipulator, thus being inserted perpendicularly to S1

247 cortex surface. Figure 2 outlines the various parts of the signal acquisition setup during our
248 experiment.

249 LFPs were evoked by single whiskers mechanical stimulation performed with a custom–
250 made speaker that provides dorsal–ventral movements through a connected tube. The speaker
251 was driven by a waveform generator (Agilent 33250A 80 MHz, Agilent Technologies) providing
252 1 ms, 10 V square stimuli with 150 ms delay. Each whisker, starting from the posterior group,
253 was individually inserted into the tube and the corresponding response was checked at $-750\ \mu\text{m}$
254 depth (cortical layer IV), in order to find the most responsive whisker for the selected recording
255 point in the cortex. The so–called “principal whisker” was then chosen for the recording, and the
256 evoked LFPs are recorded from all the cortical layers with a $90\ \mu\text{m}$ recording pitch. For each
257 depth, 100 single LFPs with 500 ms duration were recorded at 20 kHz sampling rate. An open
258 source software, ‘WinWCP’ (Version: 4.1.0) developed by the SIPBS, University of Strathclyde,
259 UK (http://spider.science.strath.ac.uk/sipbs/software_ses.htm) was used for recording the signals.

260 **3. Results and discussion**

261 The method was implemented in MATLAB (Version: 7.9, release: 2009b, website:
262 <http://www.mathworks.com>). As the method was designed keeping in mind all kinds of users
263 (with or without programming experience), an easy to use Graphical User Interface (GUI) was
264 also included to encapsulate the coding for the non–programming background users. The GUI is
265 shown in figure 3.

266 To check the method’s workability it was applied on a number of datasets and the results
267 were found satisfactory except some exceptional cases, when the signal morphology was
268 completely different from that of the barrel cortex. As seen in figure 1, each depth profile or

269 dataset recorded from an experiment comprised of recordings from about 20 different cortical
270 positions, and each of them contained as many as 100 single sweep LFPs. In addition, to
271 demonstrate the distribution of single LFPs in different clusters, we also present clustering
272 results related to a representative set of single LFPs. However, the usefulness of this method is
273 evidenced through experimental findings.

274 In figure 4 we can see the raw single LFPs and their average signal (left) and the
275 estimated single LFPs and their average signal (right). The arrow indicates the stimulus-onset
276 which is the starting point of the template. The main reasons behind performing the estimation
277 are two folds. Firstly, reduction of noise and oscillations without filtering out vital signal
278 information; secondly, as the single sweep signals contain heavy oscillations, the signal
279 characteristics (E1–E4) are often hidden. Thus, the smoothing facilitates the recognition of these
280 events to be used as the basis for generating the feature vector for the *iK*-means clustering.

281 After generation of the template, each single sweep signals were truncated to the size of
282 the template. This was done to facilitate the recognition process as each single sweep signal was
283 checked for their conformity within the specified bounding conditions. The figure 5 shows the
284 single LFPs truncated and zero-padded to the size of the template (in blue), the upper and lower
285 bounds of the template (in green), and the template itself (in red). We can also see the recognized
286 signals which were within the upper and lower bounds. The classification method provided two
287 means to perform the signal recognition: Contour Matching, and Matched Filter. The method
288 was applied on a dataset using both the methods. When compared, the results of the single sweep
289 recognition varied for both the methods as reported in figure 6. In case of the signals recorded
290 from the upper cortical layers (layer I and II) the matched filter could recognize more signals, but

291 in general the contour matching method provided a better signal recognition considering all the
292 recording positions.

293 The N recognized single LFPs, each represented by 200 feature points, generate a feature
294 matrix of size $200 \times N$. The features of each single sweep were selected based on the detected
295 events (E1–E4, see Section 1, paragraph 4) in combination with the stimulus–onset and the end
296 of response. Within the range of these six points 194 more points were selected. To retain more
297 information regarding the signal shape, relatively more points were selected near the events’
298 peaks than in distant locations (in a range of ± 5 ms from each event’s peak one point every 250
299 μ s was selected). Furthermore, clustering with a feature matrix of size $400 \times N$ was also done
300 and not much difference in terms of signal classification was noticed. This feature matrix was
301 then classified using the *iK*–means clustering and the result on a representative dataset is shown
302 in figure 7. In the figure we can see that the single LFPs were classified as per their shape into
303 seven different clusters, also, the averages (in red) of each cluster contained significant shape
304 difference.

305 To check the automatic and intelligent assignment of the total cluster number by the
306 method, we tabulated in Table I the recording depths, total number of recognized signals, and
307 single sweep distribution among different clusters. This table shows that the feature matrix was
308 well classified into different clusters using the *iK*–means clustering.

309 Once the single sweep clusters were formed, the program computed local averages of
310 each cluster for further processing. Analyses of these local averages (e.g., event latency, and
311 amplitude calculation) have revealed that the underlying neuronal network generating the signal
312 may be different even if we are recording signals from the same recording site under the same

313 stimulus. Figures 8 and 9 show different latencies and amplitude differences calculated from the
314 various clusters' local averages. These differences in latencies and amplitudes clearly specify the
315 shape variations of among the local averages.

316 Also, the latencies and amplitudes of E2 in each recognized and clustered single LFPs
317 were calculated. The mean latencies and amplitudes of the E2 among different clusters showed
318 variations as seen in figure 10. The variations may as well indicate that the signals were recorded
319 from neuronal populations of different distance from the recording electrode. As the position of
320 the recording electrode was fixed, we may conclude that the signals were generated by activation
321 of different neuronal networks close to the recording electrode.

322 Basing on these evidences, we can assert that the automated method can cluster the single
323 sweep LFPs successfully basing on their different shapes. The results on the latency and
324 amplitude of local averages and individual clusters demonstrate the reliability and usefulness of
325 the method.

326 **4. Conclusions**

327 Through whisking rats perform very fine discrimination of the environment. To better
328 understand the tactile information processing pathway, scientists frequently rely on LFPs as their
329 shapes work as 'fingerprints' of the neural network activities near the recording electrode. To
330 assess multiple networks' activity at one position, it is necessary to distinguish between the
331 different shapes of signals recorded at a single recording site. Till date scientists have relied on
332 single conventional average. Based on previous work and on results presented in this paper, it
333 can be seen that under the same stimulation condition different signal processing pathways can
334 get activated within the neuronal networks close to the recording electrode. Our automated

335 detection method will therefore facilitate the dissection of real network activity from averaged
336 responses. This module is a part of the SigMate software package, which will soon be made
337 available to the research community [15].

338

339 **ACKNOWLEDGMENTS**

340 This work was carried out as a part of the European Commission funded CyberRat project under
341 the Seventh Framework Programme (ICT-2007.8.3 Bio-ICT convergence, 216528, CyberRat).

342

343 **REFERENCES**

- 344 [1] M. Maschietto, M. Mahmud, S. Girardi and S. Vassanelli, “A high resolution bi-directional
345 communication through a brain-chip interface,” *Proc. of 2009 ECSIS Symp. on Advanced
346 Technologies for Enhanced Quality of Life (AT-EQUAL 2009)*, 1: 32-35, 2009.
- 347 [2] A. Legatt, J. Arezzo and H. G. Vaughan, “Averaged multiple unit activity as an estimate of
348 phasic changes in local neuronal activity: effects of volume-conducted potentials,” *J.
349 Neurosci. Methods*, 2(2): 203-217, 1980.
- 350 [3] J. van Hemmen and R. Ritz, “Neural coding: A theoretical vista of mechanisms, techniques,
351 and applications,” in: *Lecture Notes in Computer Science, Analysis of Dynamical and
352 Cognitive Systems*, S. I. Andersson (Ed.), Berlin: Springer, 75-119, 1995.
- 353 [4] M. Okun, A. Naim and I. Lampl, “The subthreshold relation between cortical local field
354 potential and neuronal firing unveiled by intracellular recordings in awake rats,” *J. Neurosci.*,
355 30(12): 4440-4448, 2010.
- 356 [5] R. Q. Quiroga, “Spike sorting,” *Scholarpedia*, 2(12): 3583, 2007. Available:
357 http://www.scholarpedia.org/article/Spike_sorting
- 358 [6] K.F. Ahrens and D. Kleinfeld, “Current flow in vibrissa motor cortex can phase-lock with
359 exploratory rhythmic whisking in rat,” *J. Neurophysiol.*, 92: 1700-1707, 2004.
- 360 [7] E. Kublik, “Contextual impact on sensory processing at the barrel cortex of awake rat,” *Acta.
361 Neurobiol. Exp.*, 64: 229-238, 2004.
- 362 [8] M. Mahmud, A. Bertoldo, M. Maschietto, S. Girardi and S. Vassanelli, “An automated
363 method for detection of layer activation order in information processing pathway of rat
364 barrel cortex under mechanical whisker stimulation,” *J. Neurosci. Methods*, 196(1): 141-150,
365 2011.

- 366 [9] M. Mahmud, D. Travalin, A. Bertoldo, S. Girardi, M. Maschietto, and S. Vassanelli, “An
367 automated method for clustering single sweep local field potentials recorded from rat barrel
368 cortex,” *Proc. ISSNIP Biosignals and Biorobotics Conf. 2011*, 1: 1-5, 2011.
- 369 [10] K. Madsen and H. B. Nielsen and O. Tingleff, *Methods for Non-Linear Least Squares*
370 *Problems (2nd ed.)*, Kgs. Lyngby: Informatics and Mathematical Modelling, Technical
371 University of Denmark (DTU), 2004.
- 372 [11] J. Macqueen, “Some methods for classification and analysis of multivariate observations,”
373 *Proc. Fifth Berkeley Symp. on Math. Statist. and Prob.*, 1: 281-297, 1967.
- 374 [12] H. H. Bock, “Clustering methods: a history of K-Means algorithms,” in: *Selected*
375 *contributions in data analysis and classification*, P.D. Brito, G. Cucumel, F. de Carvalho
376 (Eds.), Heidelberg: Springer Verlag, 161-172, 2007.
- 377 [13] M. M. T. Chiang and B. Mirkin, “Intelligent choice of the number of clusters in K-means
378 clustering: an experimental study with different cluster spreads,” *J. Classif.*, 27(1): 3-40,
379 2010.
- 380 [14] L.W. Swanson, *Brain Maps: Structure of the Rat Brain*, London: Academic Press, 2003.
- 381 [15] M. Mahmud, A. Bertoldo, M. Maschietto, S. Girardi and S. Vassanelli, “SigMate: A
382 MATLAB-based neuronal signal processing tool,” *Conf. Proc. IEEE Eng. Med. Biol. Soc.*, 1:
383 1352-1355, 2010.
- 384

385 **FIGURE CAPTIONS**

386 Figure 1: Depth profile of LFPs recorded from the E1 barrel column by stimulating the E1
387 whisker where the different features of the signals can be easily seen. Each LFP shown
388 here is average of 100 single signals.

389 Figure 2: Signal acquisition setup showing its different components (top). The stimulus is shown
390 at the bottom which is used in driving the speaker.

391 Figure 3: The GUI of the LFP sorting method with its components. The plotted 100 single sweep
392 LFPs of a recording session give an idea about the varied shapes that may be present in
393 recordings.

394 Figure 4: Single LFPs: on left, raw LFPs without smoothing or estimation with average (in red)
395 and on right, estimated LFPs with average (in red). The arrow shows the stimulus–
396 onset i.e., the starting point of the template. The noise in the raw single LFPs is evident
397 in the left figure.

398 Figure 5: The template (in red), the upper and lower bounds (in green), and the single LFPs
399 truncated to the size of the template (in blue). Also the recognized single signals whose
400 data points fall within the bounds can be seen.

401 Figure 6: Comparison of single sweep matching using contour matching method and matched
402 filter method.

403 Figure 7: Clustering result using *iK*–means clustering method. Single LFPs (in blue) and their
404 respective averages (in red) depict clear differences in the shapes among signals of
405 different clusters.

406 Figure 8: Latency variation among different clusters local averages. Each bar corresponds to a
407 local average of a cluster and each color corresponds to a recording depth consisting of
408 a number of clusters.

409 Figure 9: Amplitude variation among different clusters local averages.

410 Figure 10: Cluster-wise mean latency (top) and mean amplitude (bottom) of signals recorded
411 from 720 μm . The error bars indicate the standard deviation.

412

413

414 **TABLE CAPTIONS**

415 Table I: Total recognized single LFPs, and single sweep allocation to different clusters. "--"
416 denotes no clusters.

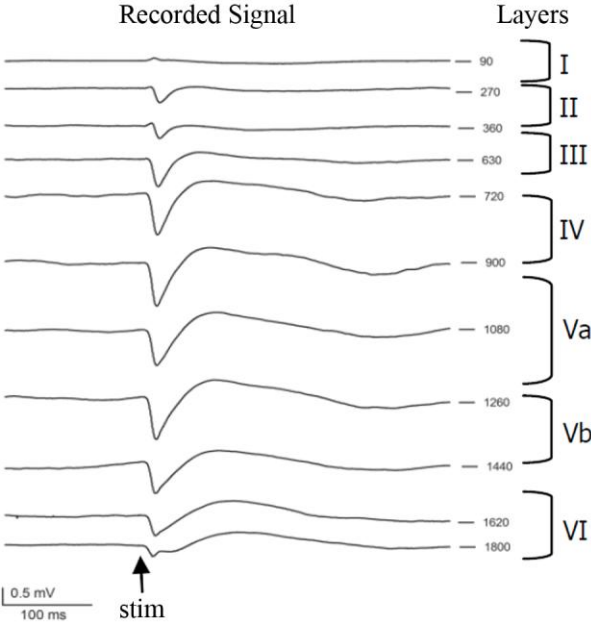
417

418

419 **Figures:**

420 **Figure 1**

421



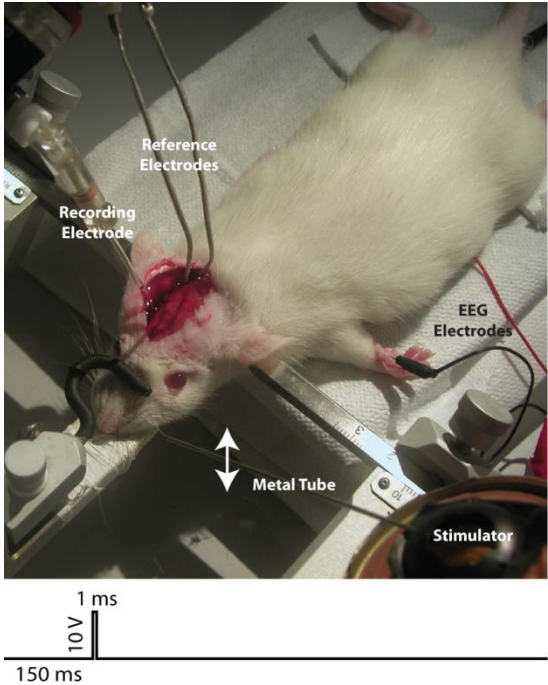
422

423

424

425

Figure 2



426

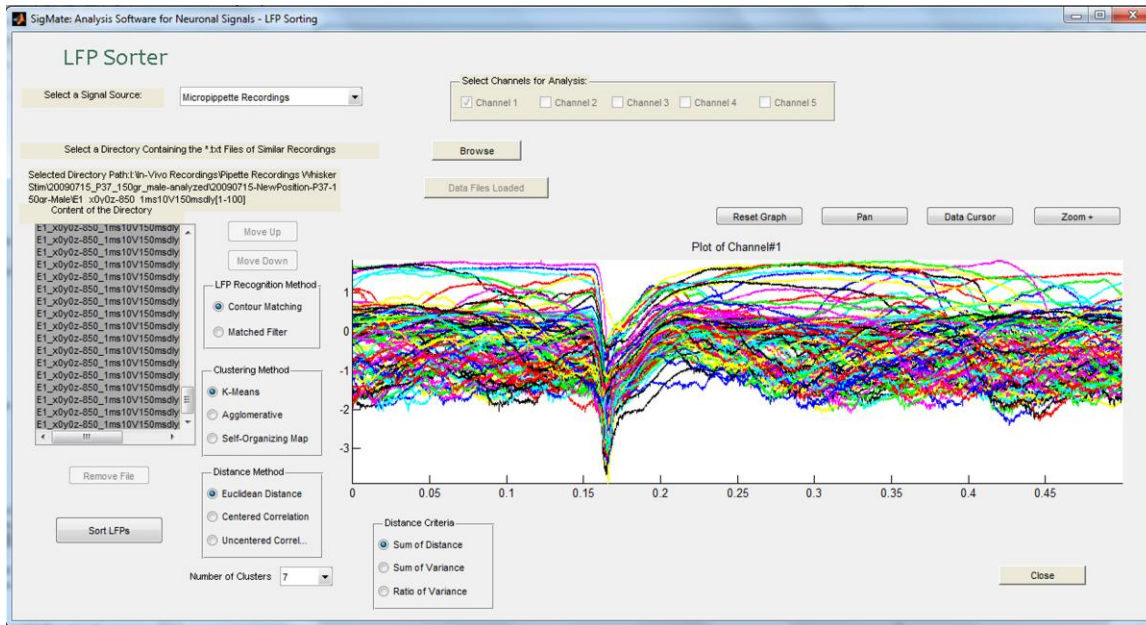
427

428

429

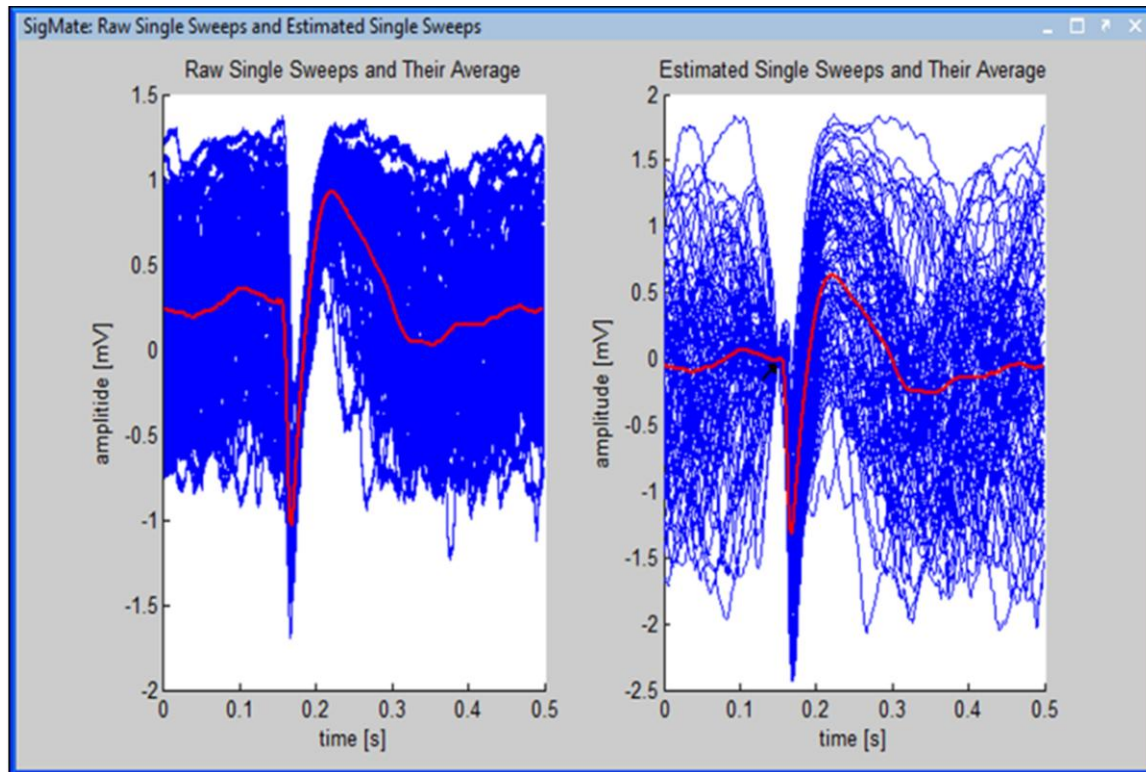
430
431
432
433

Figure 3



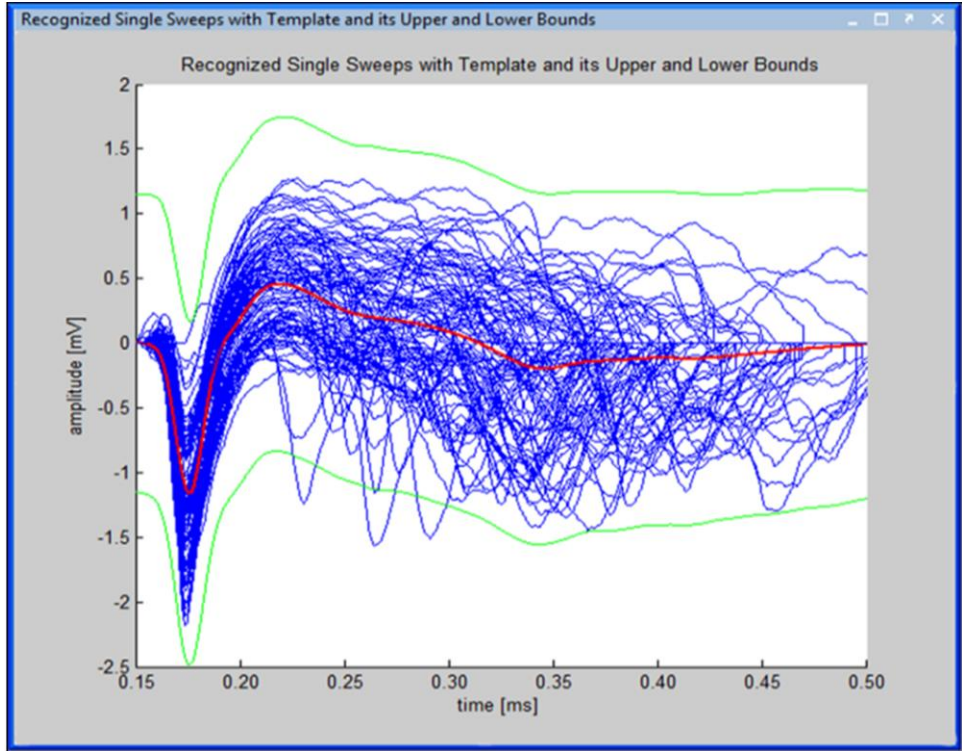
434
435
436
437

Figure 4



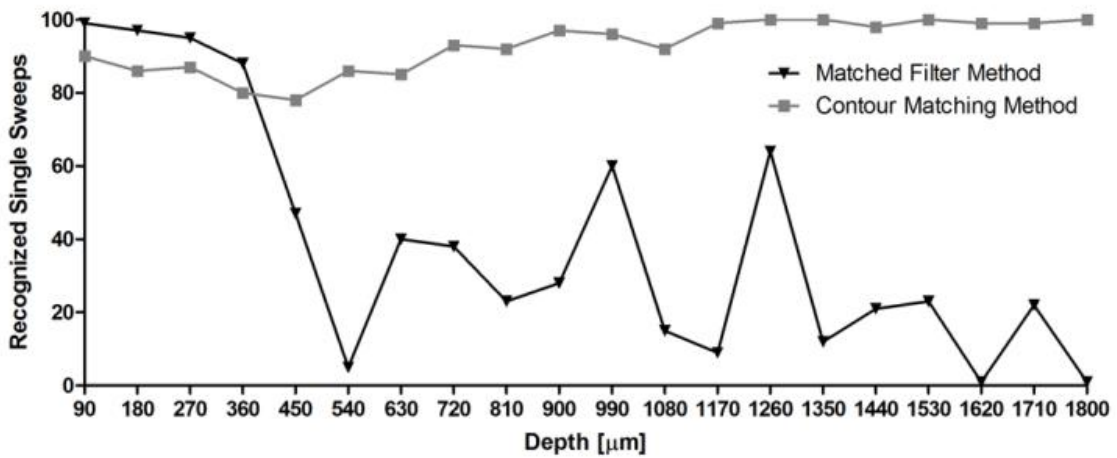
438
439
440

441 **Figure 5**
442



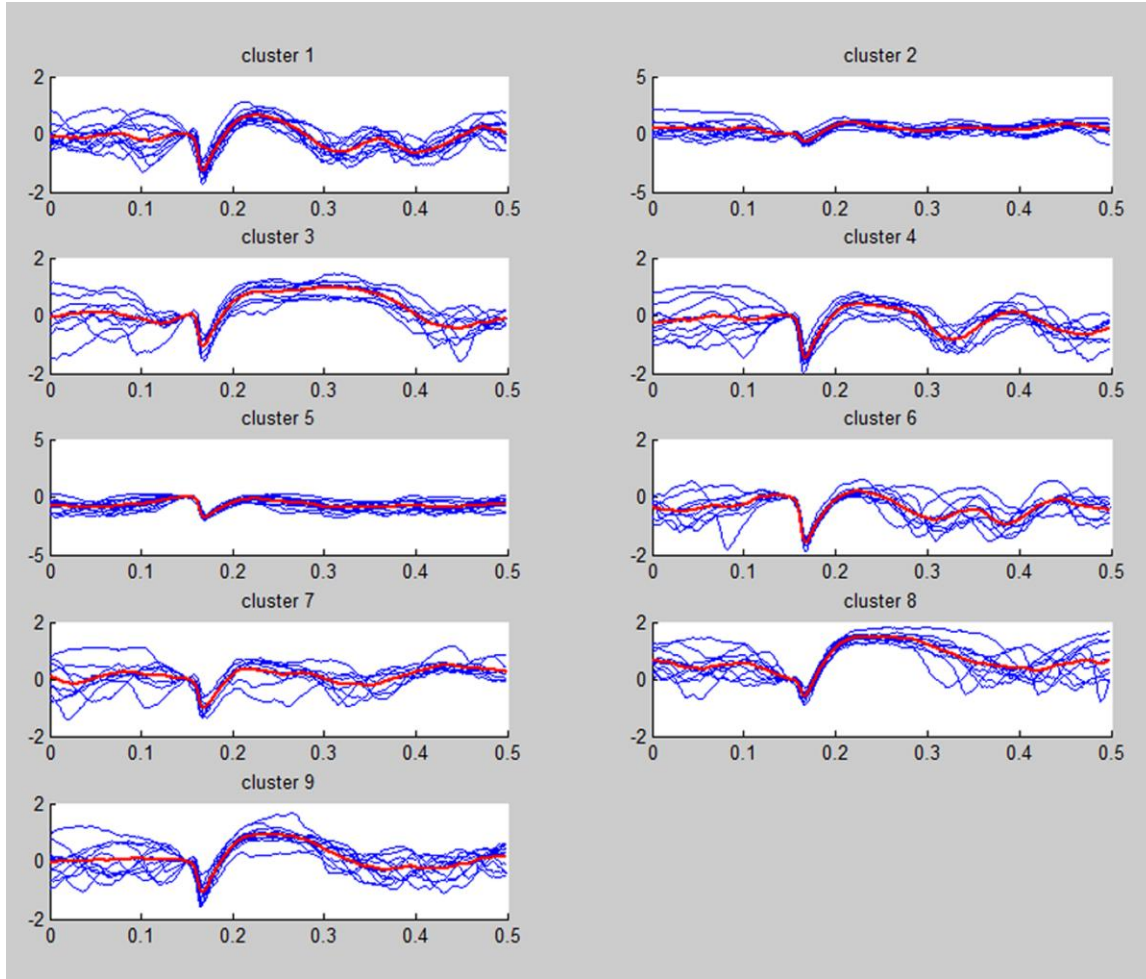
443
444
445
446
447
448

Figure 6

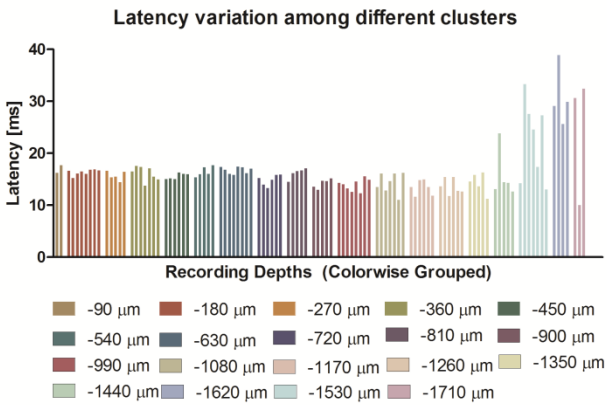


449
450
451
452
453
454
455

456 **Figure 7**
457

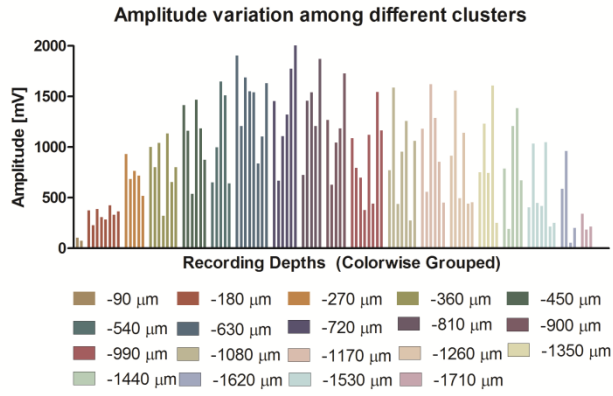


458
459
460
461 **Figure 8**
462

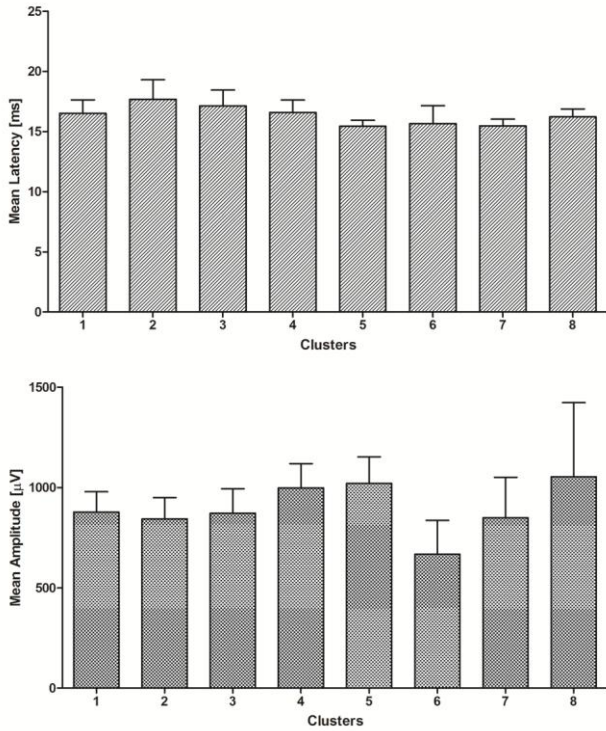


463
464
465

466 **Figure 9**
467



468
469
470 **Figure 10**
471



472

473
474
475
476
477
478
479

480 **Tables:**

481

482 **Table I**

483

Recording Depth [μm]	Recognized Single LFPs	Clusters Numbers									
		1	2	3	4	5	6	7	8	9	10
90	90	5	6	12	11	11	7	8	12	6	12
180	86	11	17	10	17	18	13	--	--	--	--
270	87	8	8	8	11	15	7	4	10	10	6
360	80	7	10	7	10	13	9	11	9	--	--
450	78	10	9	11	4	7	15	9	13	--	--
540	86	9	8	16	9	9	2	9	8	7	9
630	85	16	6	15	14	17	17	--	--	--	--
720	93	6	18	17	16	7	16	13	--	--	--
810	92	10	9	13	9	13	8	14	6	10	--
900	97	11	15	6	8	14	10	6	9	9	9
990	96	19	15	15	10	5	17	15	--	--	--
1080	92	12	12	9	9	12	9	8	10	11	--
1170	99	8	13	13	9	6	11	10	9	10	10
1260	100	11	20	13	16	7	7	16	10	--	--
1350	100	18	13	19	19	19	12	--	--	--	--
1440	98	13	10	16	8	16	14	7	5	9	--
1530	100	7	9	18	7	14	7	10	16	12	--
1620	99	10	5	16	10	11	8	10	12	11	6
1710	99	10	12	20	13	14	12	18	--	--	--
1800	100	10	12	5	15	16	14	9	19	--	--

484